doi:10.5697/oc.55-3.573
OCEANOLOGIA, 55 (3), 2013.
pp. 573–597.

KEYWORDS
Aerosol number concentration
Principal component analysis
Wavelet transform
Coastal site
source apportionment

Observations of the aerosol particle number concentration in the marine boundary layer over the south-eastern Baltic Sea*

Steigvile Byčenkienė
Vidmantas Ulevicius⋆
Nina Prokopčiuk
Dalia Jasinevičienė

Centre for Physical Sciences and Technology,
Savanoriu pr. 231, LT–02300 Vilnius, Lithuania;

e-mail: ulevicv@ktl.mii.lt

⋆corresponding author

Received 28 January 2013, revised 29 March 2013, accepted 23 April 2013.

Abstract

Continuous measurements of the aerosol particle number concentration (PNC) in the size range from 4.5 nm to 2 μm were performed at the Preila marine background site during 2008–2009. The concentration maxima in summer was twice the average (2650 ± 850 cm^{-3}). A trajectory-based approach was applied for source identification. Potential Source Contribution Function (PSCF) analysis was performed to estimate the possible contribution of long-range and local PNC transport to PNC concentrations recorded at the marine background site. The PSCF results showed that the marine boundary layer was not seriously affected by long-range transport, but that local transport of air pollution was recognized

* The research leading to these results has received funding from Lithuanian-Swiss cooperation programme to reduce economic and social disparities within the enlarged European Union under project AEROLIT agreement No. CH-3-ŠMM-01/08.

as an important factor. North Atlantic and Sea-Marine type clusters respectively represented 32.1% and 17.9% of the total PNC spectra and were characterized by the lowest PNCs ($1\,080 \pm 1\,340$ and $1\,210 \pm 1\,040$ cm^{-3} respectively) among all clusters.

Wavelet transformation analysis of 1-h aerosol PNC indicated that while the 16-h scale was a constant feature of aerosol PNC evolution in spring, the longer ($\sim$60-h) scales appeared mainly over the whole year (except June). Principal component analysis (PCA) revealed a strong correlation between PNC and NaCl, highlighting the influence of sea-salt aerosols. In addition, PCA also showed that PNC depended on optical and meteorological parameters such as UVR and temperature.

1. Introduction

In recent decades, atmospheric research has focused on the global distribution of atmospheric aerosol particles because of their effects on the global and regional climate and the environment. Particulate matter (PM) can also exert an influence: it affects the Earth's radiation budget directly by absorbing and scattering light, and indirectly by acting as cloud condensation nuclei (Lohmann & Feichter 2005). Recently, numerous epidemiological and toxicological studies have addressed the association between the PM concentration and the negative health risk due to ultrafine particles (UFP, particle diameter Dp < 0.1 μm) compared to particles of greater diameters (Englert 2004, Xia et al. 2006, Gong et al. 2006, Delfino et al. 2009). The marine aerosol constitutes one of the most important natural aerosol systems globally. Recent measurements indicate the existence of many submicron and ultrafine-mode (< 0.1 μm) sea-salt aerosol particles that dominate the aerosol particle number concentration (PNC) in the marine environment (Clarke et al. 2006). In view of recent interest in the effects of anthropogenic aerosols on marine clouds and precipitation, the number concentration of marine aerosol particles assumes an important role as a property of the background aerosol to which the influence of anthropogenic aerosols are to be compared.

Although the current National Ambient Air Quality standards for PM (based on PM2.5 and PM10) are mass-based, there is increasing evidence that a number-based standard for both climate and air quality studies is often a more pertinent parameter for UFP concentrations (Englert 2004) due to the fact that the UFP number concentration is dominated by its fine fractions, the UFP fractions in particular (Hinds 2009). In ambient air UFPs are present in very high numbers – on average of the order of 10^4–10^5 particles cm^{-3} in urban areas – but contribute only a few per cent to the overall PM mass. Moreover, PM2.5 concentrations are often used as a surrogate for UFP mass concentrations (Wilson & Zawar-Reza 2007),

whereas a poor correlation has been found between the UFP number and PM2.5 mass concentrations (Sardar et al. 2004, Rodriguez et al. 2005).

Seasonal and diurnal variations of aerosol PM2.5 and PM10 mass concentrations have been extensively documented in various environments (Putaud et al. 2004, Karaca et al. 2005, Ho et al. 2006, Dongarrá et al. 2010, Saliba et al. 2010). Although it was declared that the aerosol number concentration might be a better indicator of health effects of particulates than the mass-based method, there is a lack of aerosol number investigations. The Lithuanian National Air Quality Monitoring Network does not carry out aerosol number concentration measurements. Nonetheless, for decades in Lithuania the focus has been on the physical and optical properties (Ulevicius et al. 2010, Plauškaitė et al. 2010) of aerosols such as the mass concentration, but only a small number of continuous measurement studies have been performed in the eastern Baltic compared to the number concentration dynamics of ambient particulate matter. There is therefore a need to study the processes controlling the dynamics of aerosol number concentration in this background marine area. The present work is a continuation of our efforts to analyse particle number concentration dynamics (Juozaitis et al. 1996, Ulevicius et al. 2001, Plauškaitė et al. 2010) in the south-eastern Baltic Sea.

In the atmosphere, the aerosol PNC is highly variable in time and space owing to physical and chemical processes such as particle production and consumption by chemical reactions, condensation growth or phase transitions. Typical air quality time series reveal periodic behaviour (hourly, daily, weekly, seasonal, yearly) caused by the meteorological situation and anthropogenic sources. Changing meteorological conditions, resulting from the presence of a nearly stagnant high-pressure system or the passage of frontal systems, cause the aerosol number concentration to vary on a synoptic scale. Baseline fluctuations are expected to be caused by such processes as the seasonal variations of the solar flux that change large-scale flow patterns. Large data sets usually contain a huge amount of information, which is often too complex for straightforward interpretation. Principal Component Analysis, Fourier and wavelet transform (WT) are methods that help to extract more information from a data set than when individual parameter analysis is used. These analyses, based on PCA, wavelet and Fourier transforms, are used to characterize time series in the frequency domain and to study the periodicities hidden in the data (Eskridge et al. 1997, Hies et al. 2000, Marr & Harley 2002). Standard principal component analysis was developed largely for handling social science data and has been used mainly for source identification and apportionment. The Fourier transform allows us to determine different frequency bands

in the analysed data domain and helps to understand various underlying processes related to aerosol PNC fluctuations (Percival & Walden 2008). Wavelet transform methods have found wide application in various fields of science, including meteorology and oceanography (Foufoula-Georgiou & Kumar 1995, Torrence & Compo 1998). The dissimilarity between these two kinds of transform is that the individual wavelet functions are localized in space. The wavelet theory can be viewed as an extension of the Fourier theory and provides a flexible alternative to the Fourier method in non-stationary signal analysis.

While the continuous time series is obtained as 1-h and 24-h series of the average aerosol particle number concentration at a fixed location, its analysis highlights a series of features that have not been investigated before. To better understand the variability and climatic role of aerosols in the south-eastern Baltic Sea region, intensive measurements of atmospheric aerosol particles were conducted at a background marine site in 2008–2009. The aim of this paper is to investigate the factors influencing PNC concentrations in a marine background environment by applying the k-clustering method, Principal Component Analysis, and wavelet and Fourier transforms to aerosol number concentration data and to state the results obtained by these techniques.

2. Material and methods

2.1. Site description and instrumentation

The aerosol PNC measurements were performed at the EMEP Preila environmental pollution research station (55°55′N, 21°00′E, 5 m above sea level) in a coastal/marine environment. Located on the Curonian Spit, which separates the Curonian Lagoon and the Baltic Sea, this station can be regarded as a regionally representative background area (Figure 1).

In Lithuanian conditions, there are several important phenomena governing aerosol particle number concentrations. The first one is long-range transport (Andriejauskienė et al. 2008). If the air masses come from areas with high emission levels, the air parcels contain more particles (Kulmala et al. 2000). Secondly, in addition to the primary or direct emissions, photochemical reactions in the atmosphere may also be responsible for the formation of secondary ultrafine particles (Kulmala et al. 2004). Their long-range transport as well as photochemical particle formation in the atmosphere can lead to elevated PNC (Verma et al. 2009). Thirdly, weather and season affect emissions and aerosol PNC, for example, as a result of springtime wildfires (Ulevicius et al. 2010) or sea spray.

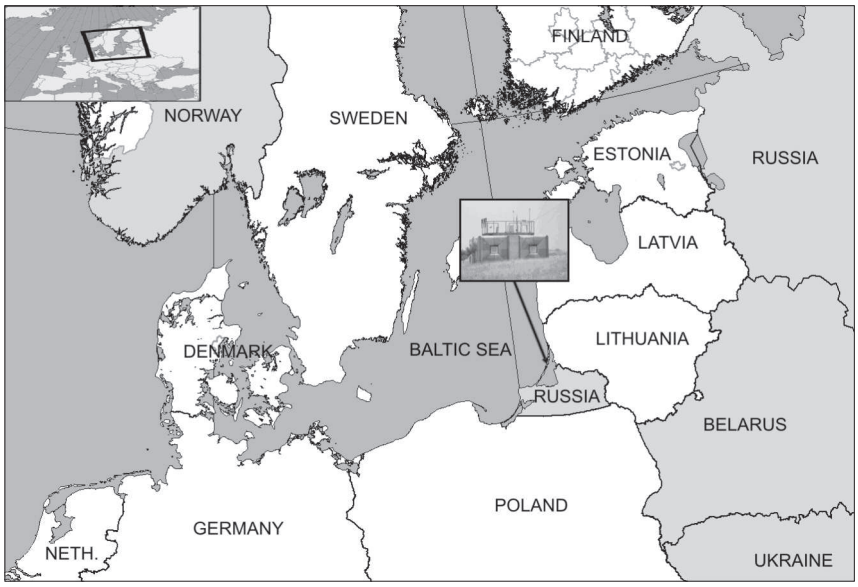

Figure 1. The location of the observation site

For the 2008–2009 period, the aerosol PNC was measured continuously using a condensation particle counter (CPC) UF-02 (Mordas et al. 2005). The CPC was designed to detect ultrafine aerosol particles of a few nanometres with high efficiency. The design of the instrument is based on the swirling flow generated inside the saturator (43°C) – condenser (10°C). The instrument uses a high carrier flow rate (1 l min^{-1}). The aerosol flow (0.27 l min^{-1}) is extracted from the carrier flow by a capillary. This aerosol flow is divided into two. The first one (0.03 l min^{-1}) is directed to the condenser. The second flow (0.24 l min^{-1}) is circulated through a HEPA filter and a saturator block, in which the flow is saturated with respect to n-butanol and then mixed with the aerosol-laden air in a cooled condenser. This mixing generates a supersaturated region with respect to n-butanol. The butanol vapour condenses on the particles, which act as condensation nuclei. This process increases the size of each individual nanoparticle. Such large droplets can be conveniently detected by light scattering.

The lower cut-off size of the CPC, i.e. the limiting size when 50% of the particles are successfully accounted for, is determined to be 4.35–4.46 nm. The instrument is fitted with an impactor (laminar flow, nozzle diameter = 7.4 mm) to reduce the influence of large particles. Annual maintenance involves CPC calibration and thorough cleaning.

Other data, including mass concentrations of trace gases and meteorological parameters (temperature, relative humidity, wind speed and wind

direction (T, RH, WS and WD respectively)), were obtained from the Preila station EMEP measurement database. Air samples were collected for a 24 h period using filter-packs and analysed for water-soluble ions: ($SO_4{}^{2-}$, $NO_3{}^-$, Cl^-, $NH_4{}^+$, Na^+, K^+, Ca^{2+}). The anions in the samples were determined by ion chromatography (Dionex 2010i with conductivity detector; column – Ion Pac AS4A-SC; eluent – 1.8 mM sodium carbonate + 1.7 mM sodium bicarbonate; regenerant – 100 mM H_2SO_4). The Na^+, K^+ and Ca^{2+} concentrations were determined by atomic emission. Indophenol-spectrophotometry was used to determine the $NH_4{}^+$ concentration.

2.2. Clustering method

In accordance with the study of Dall'Osto et al. (2011), CPC data were analysed using k-means cluster analysis (Beddows et al. 2009). 72 h back trajectories of the air masses arriving at Preila were calculated for 12:00 UTC on each day to show the path taken by the air mass reaching the sampling site over the previous three days.

Air mass back trajectory analysis was used to determine the direction and sources of PNC at the receptor site. To calculate PSCF, the whole eastern Baltic region covered by the trajectories was divided into an array of grid cells. PSCF is a function of location as defined by the cell indices i and j, while the number of segments with endpoints that fall in the ij^{th} cell is denoted by n_{ij}. The number of endpoints in the ij^{th} cell associated with a trajectory that arrives at the sampling site at the same time as a corresponding measured pollutant concentration higher than an arbitrary criterion value is defined by m_{ij}. The value of PSCF for the ij^{th} cell is then

$$\text{PSCF}_{ij} = m_{ij}/n_{ij}. \tag{1}$$

The value of PSCF was interpreted as the probability that the concentration of a given pollutant greater than the criterion level is related to the passage of an air parcel through the ij_{th} cell. These cells are indicative of areas of high potential contributions for that pollutant.

The contribution of each source group (cluster) to the aerosol number concentration was quantitatively assessed by means of multiple linear regression analysis (MLRA). MLRA was applied to the data, using PNC as the dependent variable and the compounds that had the highest factor loadings in each factor as independent variables.

According to the backward trajectories, air masses arriving at Preila were classified into three main groups: Sea – Marine air type, SC – South-Continental, NA – air masses originating from the North Atlantic and NC – North Continental air masses. Because the direction of air mass transport from the Baltic Sea region is our main interest in the analysis of marine

source regions, angle distance was chosen as the clustering model. A final cluster number of 4 was selected after visual examination of the mean trajectory maps for different cluster numbers. After the cluster number identification was assigned to each trajectory, the statistical results of the mean concentration of all trajectories were calculated for each cluster.

2.3. Statistical investigation of the aerosol particle number concentration

Since the direct assessment method of spectral density is based on an infinite series consisting of the square module of the fractional Fourier transform, the use of average values does not always lead quickly to an appropriate result. Therefore, non-parametric (the so-called classical) methods are usually applied to the spectral density assessment. The idea of the basic Fourier transform (FT) is to write down a function $f(x)$ as the summation of a series of sine and cosine terms of increasing frequency. The Fourier transform is very commonly applied to atmospheric time series, and important conclusions can be drawn in the frequency domain. These methods represent time series data in terms of contributions occurring on different time scales or at characteristic frequencies. Fourier analysis includes transformation of the original data (y_t) into coefficients that multiply an equal number of the periodic data. The Fourier transform is defined by equation 2:

$$y_t = \overline{y} + \sum_{k=1}^{\infty} A_k \cos\left[\frac{2\pi kt}{T}\right] + B_k \sin\left[\frac{2\pi kt}{T}\right], \tag{2}$$

where T is the measurement period, A_k and B_k are the Fourier coefficients, t is the time and k is the harmonic number.

Another method for analysing time series with regard to typical time scales utilizes the wavelet transformation (WT), which decomposes the signal into a time-frequency space. Both methods have great potential for revealing the temporal variability of aerosol number concentrations, and for evaluating their spectral similarity with respect to other turbulent scalars. While WT decomposition can also be carried out using Fourier analysis, there is a fundamental difference between WT and Fourier analysis. Fourier analysis represents a signal at all frequencies or length scales, whereas wavelet analysis provides both the spatial and frequency aspects of a signal.

In this work we used the most common Morlet wave, which is defined as the product of the complex sinusoid and Gaussian curve:

$$\psi_0(\eta) = \pi^{\frac{-1}{4}} e^{iw_0\eta^2} e^{\frac{\eta^2}{2}}, \tag{3}$$

where η is a non-dimensional time parameter and w_0 is the non-dimensional frequency (assumed equal to 6 to guarantee admissibility of the function) (Farge 2000). Given the time series of aerosol particle number concentration x_i with $i = 0, \ldots, N-1$, the wavelet transform reads

$$W_n(s) = \sum_{n'=0}^{N-1} x_{n'} \psi^* [\frac{(n'-n)\delta}{s}], \tag{4}$$

where * indicates the complex conjugation of the wavelet function, s is the 'dilation' parameter used to change the scale, and n and n' are the translation parameters used to slide in time.

The two-dimensional view of such a variation is obtained by plotting the wavelet amplitude

$$|W_n(s)| = \sqrt{\{\mathrm{Re}[W_n(s)]\}^2 + \{\mathrm{Im}[W_n(s)]\}^2}, \tag{5}$$

where Re is the real part and Im is the imaginary part of the Morlet wavelet.

The inverse tangent of its imaginary-to-real part ratio thus denotes the desired phase:

$$\varphi_n = \tan^{-1}\{\mathrm{Im}[W_n(s)]/\mathrm{Re}[W_n(s)]\}. \tag{6}$$

PCA is a special case of factor analysis that transforms the original set of intercorrelated variables into a set of uncorrelated variables. It is a method that helps extract more information from a time-series than when individual parameter analysis is used (Fahrmeir et al. 1996, Einax et al. 1997). It extracts the directions in which a cloud of data points is maximally stretched, i.e. has maximal variance. The most relevant information of the data set (J variables with K observations) is contained in these directions (i.e. principal components (PCs)). The PCs represent orthogonal and therefore independent linear combinations PC_i of the J original variables v

$$\mathrm{PC}_{(i)} = \sum_{j=1}^{j-1} b_{ij} v_j, \tag{7}$$

where b_{ij} are the component loadings and indicate how strongly a specific original variable v_j contributes to PC_i, and v_j is the original variable. PCs are found by calculating the eigenvectors and eigenvalues of the data covariance matrix. The projection of the original data on the eigenvectors defines the PCs, and the eigenvalue of every eigenvector indicates the contribution of the specific PC to the total data set variance. There are several equivalent ways of deriving the principal components mathematically. The simplest one is to find the projections which maximize the variance. The first PC is the direction in feature space along which

projections have the largest variance. PC2 is the direction which maximizes variance among all directions orthogonal to the first. PC1 carries most of the information about the data (i.e. explains most of the variance in the data), PC2 will then carry the maximum residual information, and so on. Here, multivariate data analysis was applied to the data set to quantify their contribution to variation in the measured chemical composition and meteorological parameters.

2.4. Significance levels

Some of the time series are generally noisy, complex and non-stationary. Wavelet analysis was used to overcome this problem. It is known that geophysical time series can be modelled as either white noise (with a flat Fourier spectrum) or red noise (increasing power with decreasing frequency). A simple model for red noise is the univariate lag^{-1} autoregressive AR(1). Thus the greatest value of the power, lying within the 95% range of connected domains of reliability, was calculated under the assumption that the random component is Gaussian white noise or red noise by a factor autocorrelation at lag unit step $\alpha = 0.6$. If the power of the detected wavelet signal was higher than expected (e.g. over the 95th percentile) for such AR(1) noise, the signal was assumed to have not originated from random oscillations in the atmosphere.

3. Results and discussion

The results are divided into several sections, including (a) the summary statistics, (b) the clustering and potential source contribution function and the spectral analysis of aerosol PNC time-series, and (c) the PCA method. In these sections the aerosol particle number concentration time-series are analysed by the methods described in section 2.

3.1. Summary statistics

The results discussed in this study cover the data acquired from 2008 to 2009. The various descriptive statistics regarding the measured aerosol PNC distributions are depicted in Figure 2.

During the entire study period, there were several pronounced increases in aerosol number concentration. It follows from Figure 2 that the highest values were recorded during April–September of 2008 and 2009; the monthly mean aerosol PNC varied from $1\,500 \pm 900$ (November) to $4\,500 \pm 900$ cm^{-3} (June) in 2008 and from $1\,520 \pm 910$ (January) to $3\,830 \pm 1\,760$ cm^{-3} (September) in 2009.

The maximum daily mean concentration during the whole measurement period was recorded in April 2008 ($12\,500$ cm^{-3}) and the minimum in August

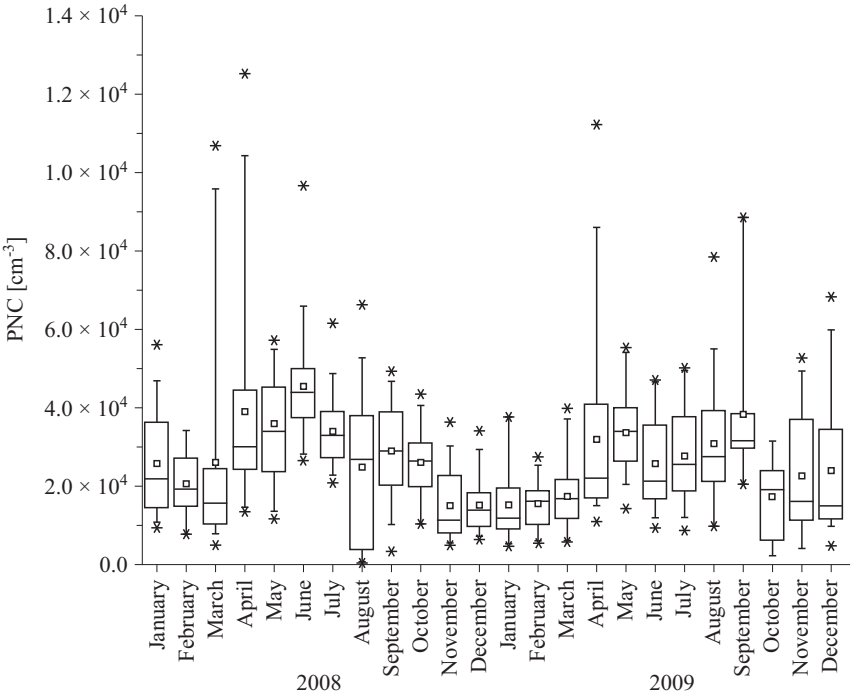

Figure 2. Box plots of aerosol particle number concentration. The horizontal lines in the box denote the 25th, 50th and 75th percentiles. The error bars denote the 5th and 95th percentiles. The asterisk below the 5th percentile error bar denotes the minimum value and the one above the 95th percentile error bar denotes the maximum value. The square symbol in the box denotes the monthly mean of the number concentration

2008 (40 cm^{-3}). During the cold season, when the air temperature dropped below zero, a higher aerosol PNC was usually observed (October–March). This is explained by the use of fossil fuels and biofuels for home heating. The studies by Jayaratne & Verna (2001) indicate that the domestic use of fossil fuels and biofuels could be a major source of aerosol particles. The spring peaks (in both 2008 and 2009) are evident; the long-range or regional movement of smoke emitted as a result of biomass burning had a strong impact on the total aerosol number concentrations in Lithuania over this period (Ulevicius et al. 2010, Byčenkienė et al. 2011). Here, the close association between particle mass and number concentration may support the hypothesis that vehicular emission sources or combustion emissions are the major source of ultrafine particles. The maximum during spring, given that the lowest detection limit was 4.5 nm, provides an excellent opportunity for nucleation and the transport of new particles from cleaner areas (Laakso et al. 2003).

The effect of season is related to e.g. home heating, hence domestic biomass burning is a significant emission source during the winter, especially in the countryside. It is suggested that without sufficient photochemical processes in winter, weak convection in the absence of high temperatures and the stronger emission of primary particles during the heating period may promote the formation of nanoparticles. The aerosol number concentration exhibited great variability during the year. It can be seen that spring concentration maxima (up to $13\,000 \pm 980$ cm^{-3}) are ~ 4 times the average. For instance, Jaenicke (1993) gives a total PNC for remote continental areas of 6000 cm^{-3}, whereas our values at Preila are about 2650 ± 850 cm^{-3}. These results are comparable to the study done at Hyytiala (2110 cm^{-3}) (Laakso et al. 2003). Laakso et al. (2003) analysed aerosol number concentrations based on measurements made in four different places (Helsinki, Hyytiala, Pallas and Varrio) in 1999–2001 and also found that the aerosol number concentration started to increase distinctly during the spring months.

During 2009 the monthly mean aerosol number concentration started to increase in April, reaching a peak of 3830 cm^{-3} in September. Meanwhile, the hourly aerosol number concentration peaked during March and April, whereas the monthly mean was recorded in April and June 2008 (Figure 2). These months are associated with high aerosol particle concentration events, which last for several days. The mean aerosol PNC in April was found to be 3910 ± 2520 cm^{-3}, whereas the value of 3370 cm^{-3} was calculated by omitting high concentration event days. In 2009 the highest monthly mean was recorded in September. Changes in the aerosol PNC mean, maximum, 75th and 25th percentiles show a slightly different behaviour of peak values during the same period in 2008 and 2009. As shown in Figure 2, the aerosol particle number concentration 75th percentile declined markedly in January–March 2008. A weaker peak in autumn is thought to be weather-related, especially the mixed layer height. The frequency distribution of 24 h mean number concentrations covering the two-year sampling period is presented in Figure 3. The classes have a window size of 100 cm^{-3} (bars). The distribution can be approximated by the lognormal distribution. Up to this point we found a four-modal lognormal function to fit each of the modes in Figure 3a.

Figure 3 shows some processes along with the four number concentration ranges (modes (lines)) where high aerosol number concentrations are often observed. Interestingly, as this figure shows, the most abundant values are the lower aerosol PNC fractions of 1–2000 cm^{-3}, indicative of clean air masses and deposition. The significant contribution (the second mode) to the number distribution of concentration is representative of background and long-range transport (~ 2400 cm^{-3}). The third and fourth modes were

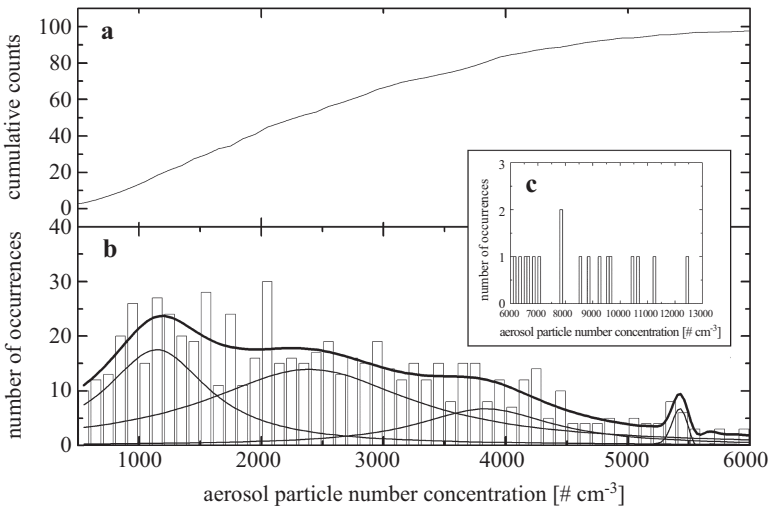

Figure 3. The frequency distribution of 24-h mean aerosol particle number concentration at Preila for the study period. The heights of the bars are proportional to the class frequencies. The plot was fitted where the highest peaks are the modes (lines)

noted within the 3800 and 5500 cm^{-3} size ranges respectively. The third mode was believed to be representative of the summer period. The spring and summer number size distributions shapes were close to those observed at Nordic stations (Aspvreten, Pallas, SMEAR II) with an almost unimodal distribution shape. The third mode is thought to represent accumulation mode concentrations (Asmi et al. 2011).

The fourth mode is believed to be composed of chemically aged aerosols occurring as a result of heterogeneous interactions between particles and gases. Furthermore, the overall PNC distribution in the high concentration modes was also found to be closely related to the number of primary particle emissions, observed under conditions where large numbers of primary soot-based particles were present (the heating season). Fourier and wavelet transformations were undertaken to investigate this matter further.

3.2. Source apportionment and contribution

Figure 4 shows the frequency of air mass trajectories affecting PNC during summer 2008. It is clear that Preila PNC was affected by South Continental (39.3%, 3340 ± 1800 cm^{-3}) and North Atlantic (32.1%, 1080 ± 1340 cm^{-3}) air masses. The backward trajectories indicate a north European (10.7%, 1760 ± 1810 cm^{-3}) origin of the air masses with final re-circulation over the sea (17.9%, 1210 ± 1040 cm^{-3}).

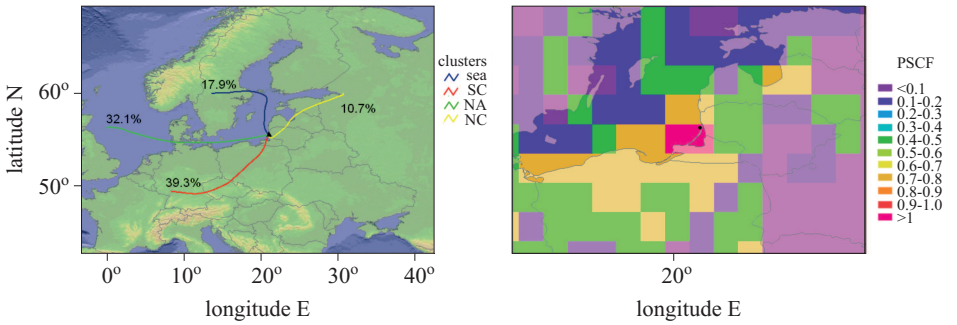

Figure 4. Potential source maps for PNC arriving at 5 m altitude in Preila during summer 2008

As the high level of variation in PNC makes it difficult to differentiate between local and long-range sources, the possible source contribution was evaluated using the PSCF model. This was run with the summer data to avoid the influence of home heating.

For the data the main part of the Baltic Sea appears to a potential source of PNC. Baltic Sea regions are important potential PNC sources with a PSCF value of around 0.6–0.8. Some regions were highlighted as making high potential contributions. These are the regions located to the west of the site. PSCF results for 5 m altitude trajectories indicate that the areas south of Kaliningrad (Russia) and north of Poland are also high potential source regions of PNC. There were fewer source potentials for 'long-range' marine regions (0.1–0.2).

In order to identify the sources contributing PNC, PCA was applied to the data using Kaiser normalization and the Varimax rotated method in SPSS statistical software packages (SPSS Inc, USA). PCA applied to PNC identified three main chemical profile sources, which accounted for 76% of the total variance. Interpretation of source profiles is based mostly on elements with factor loadings > 0.6, considered to be tracers of different sources. Table 1 lists the key results of the calculated PCA in terms of the (factor) loadings of the variables for the first three PCs. The last row in the table gives the percentage of the variance in the data that can be explained by the respective PC and the higher level PCs. PC1 explains 46% of the variance in the data, and PC2 and PC3 respectively explain 20 and 10% of the variance. PC4 to 10 are not shown because of the relatively low explanatory value of the variance.

The first PC accounted for 46% of the variance and was strongly associated with $NO_3 + HNO_3 - N$, $NO_3 - N$, $NH_4 - N$, $SO_4 - S$, $NH_4 + NH_3 - N$ and $SO_2 - S$ loadings, as well as with UVR, solar radiation and temperature, which have negative values. This suggests that this component represents

Table 1. The values of PCs and their associated variance explained by each factorial axis

	Component		
	1	2	3
$NO_3 + HNO_3 - N$	**0.913**	0.084	−0.077
$NO_3 - N$	**0.904**	0.092	−0.081
$NH_4 - N$	**0.872**	−0.274	0.078
SO−4 − S	**0.831**	0.100	0.127
$NH_4 + NH_3 - N$	**0.802**	−0.118	−0.058
$SO_2 - S$	**0.681**	−0.096	0.030
$NO_2 - N$	**0.636**	0.081	−0.211
Na^+	0.091	**0.957**	0.093
Cl^-	0.039	**0.953**	0.106
T	**−0.602**	0.02	**0.696**
RH	0.478	−0.077	−0.365
UVR(2008)	**−0.634**	0.585	0.326
solar radiation (2008)	−0.587	0.543	0.288
precipitation (2008)	0.183	**−0.643**	0.141
wind speed (2009)	0.100	**0.923**	0.223
cumulative %	**46.392**	**66.206**	**76.332**

Extraction method: Principal Component Analysis.
3 components extracted.

a general degree of pollution. A previous investigation reported that $SO_4{}^{2-}$ comes from diesel exhausts (Cheng et al. 2010), $NH_4{}^+$, $SO_4{}^{2-}$ and $NO_3{}^-$ are from secondary aerosols, while Na^+ and Cl^- are from sea spray. The only meteorological parameters that showed a noticeable loading for this PC were UVR and temperature. Moreover, PC1 was slightly negatively correlated with solar radiation, thus confirming that PNC is forced when solar radiation and its wavelength range (UVR) are low. The loadings of UVR and temperature were negative, indicating that high PNC was negatively correlated with temperature. Thus, the effect of increased PNC is enhanced by low temperature and solar radiation. Although the loadings for summer and winter were almost identical for PC1, the explained variance for the winter data (39%) was higher than that for the summer data (29%) (not shown), clearly indicating the lesser influence of combustion processes and the faster dilution of emitted particles in summer. In contrast to PC1, PC2 showed high loadings of Na^+, Cl^-, precipitation (2008) and wind speed (2009). It was surprising to find a high loading and positive correlation of wind speed in the second component. Since Cl^- is known to be a signature element of sea salt, it is in a component of its own at the Preila site, so the high loadings of Na^+ and Cl^- in PC2 could indicate the influence of high wind speeds from the Baltic Sea. Factor analysis of PM2.5 aerosol particles

collected in the Campus area by Moloi et al. (2002) showed that most of the collected PM2.5 aerosol particles at that time came from sea spray. In winter, PC3 showed a high loading only of global radiation t. In summer, the correlation with other variables was more significant. For example, PC3 correlated with the Na^+ and Cl^- concentrations with loadings > 0.5, but was negatively correlated with sulphur and nitrogen oxides.

3.3. Time-frequency analysis of aerosol number concentration

3.3.1. Periodicity analysis: periodogram

To detect common periodicities the standard Fourier transformation method of time series analysis was used. Changing meteorological conditions due to the presence of a nearly stagnant high-pressure system or the passage of frontal systems cause variations of PNC on a synoptic scale. As the aerosol concentrations vary strongly with season, especially in the Nordic countries, seasonal variability was removed from the datasets used in wavelet analysis by subtracting 15-day running average and 5 iterations from the concentrations. Later time series of 720 daily means of the aerosol number concentration were converted into the frequency domain using FT (1) and expressed by a periodogram (not shown). The dominant frequencies of the different amplitudes are the peaks of 4, 6–7, 11, 16 to 23 and 85 days. The frequencies obtained are related to the main diurnal cycles and synoptic scale oscillations. It should be noted, moreover, that short periods up to 2 days did not reflect the peculiarities of aerosol formation and sink dynamics. A range longer than 4–11 days is probably related to synoptic-scale processes, such as changes of air masses. The cause of the 23-day periodicity could be explained by the effect of synoptic-scale particle transport.

The periods of 3–5 days are close to those characteristic of the lifetime of major synoptic meteorological systems (cyclones and anticyclones). A periodicity close to a 7-day cycle is slightly perceptible, although road traffic is an insignificant parameter affecting the aerosol number concentration in Preila. This suggests that PNCs do not vary strongly with the human working week. As the characteristics of an anticyclonic system are the reverse of those of a cyclone, it is likely that the ~ 7-day period is the sum of 3 and 4 days. Longer periods are probably related to the passage of cyclones and anticyclones. In the long-term variations the frequency of the 85-day period (2–3 months) is most probably connected with large-scale weather dynamics, since the differences between the seasons are obvious in Lithuania.

The principal difference in the amplitude spectra of aerosol number and the BC concentration (Byčenkienė et al. 2011) is that the 4-, 7-, 11- and

16-day periods of PNC and BC were observed in both time-series, whereas the 3-, 29- and 63-day periods of the PNC time-series were absent. The aforementioned peculiarities of the temporal variability are evidence of some 'independence' of the PNC and the lifetime of the absorbing substance (BC) in the atmosphere. The relationship between the main periods of the PNC and BC oscillations shows that the principal circulation dynamic processes are of a similar origin.

3.3.2. Wavelet analysis

The WT approach shows how different frequencies from the aerosol number concentration change over time (Figure 5). The scalogram characterizes the signal energy on a time-scale domain.

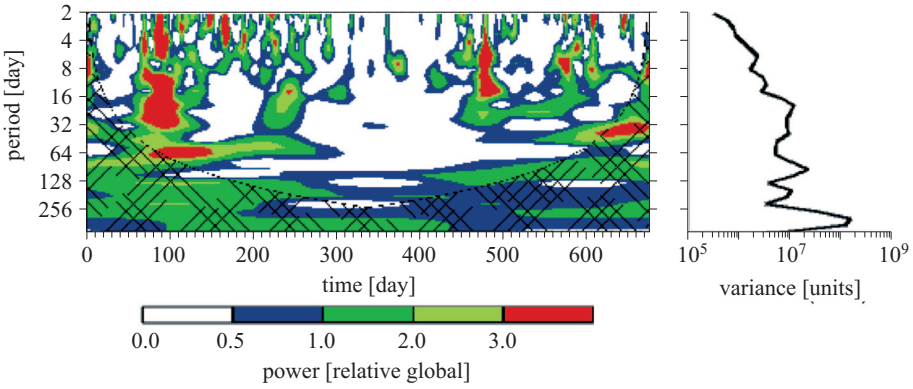

Figure 5. The wavelet power spectrum (left). The power has been scaled by the global wavelet spectrum (right). The cross-hatched region is the cone of influence (COI), where zero padding has reduced the variance

In this plot each coefficient is plotted by the gradient corresponding to the magnitude of the coefficient. The location and size of the coefficient are related to the time interval and the frequency range for this coefficient. The existence of a peak in the scalogram of a time series of the PNC indicates that a high-frequency component is present in the series. The highest amplitudes of a spectrum indicate the main periodicities of the underlying processes. Figure 5 (left) shows the wavelet analysis of the mean 1-day aerosol number concentration time series relating to the 2008–2009 period. The x-axis is the time expressed in days from the beginning of the year. The y-axis of the scalogram refers to the time scale ranging from 1 to 512 days (only large-scale details are shown at the bottom of the graph; hence, the region between 512 and 720 days is not shown). As with Fourier analysis, one can determine that the wavelet will fall within a specific range of scales

and time. The absolute value of the Fourier and wavelet transforms is not very pertinent, which is why we present the results on an arbitrary scale. Several common characteristics are worth noting, i.e. the most prominent feature of aerosol PNC data is a 1-year periodicity. The curves show a maximum that is related to the 4–6, 16–30, 80, 120, 250 and 720 day periods, which are considered to be monthly and quasi-annual oscillations.

It is evident that the periodicities obtained are dominant and well matched with the peaks exhibited by the corresponding global wavelet spectra. The approximate cyclic period of the PNC was found to be 5–6 and 16–20 days, which corresponds to the synoptic and large-scale time periods in which atmospheric high and low pressure systems interchange. It is thought that the observed frequencies could be connected with quasi-cyclic meteorological processes. Synoptic processes with periods between 8 and 11 days are known in meteorology (Vukovich 1997), and such processes could be the cause of the observed periodicities. There are reports of 30–60-day atmospheric oscillations as well (Knutson & Weickman 1987).

3.3.3. Spectral analysis of 1-h mean aerosol particle number concentration

During the study period the mean 1-day aerosol number concentration did not show any additional dynamic characteristic pattern apart from the peaks occurring during the synoptic periods, favourable meteorological conditions, air mass transport or as a result of anthropogenic influences. Comparative analysis of hourly mean data between the separate months reveals a weak 8-h periodicity in spring. Wavelet analysis (Torrence & Compo 1998) (TC98) of 1-h aerosol number concentrations (Figure 6) indicates that while the 16-h scale is a constant feature of the evolution of the aerosol PNC in spring, the longer ($\sim$60-h) scales appear mainly over the whole year (WT analysis of PNC during separate months revealed that longer ($\sim$60-h) scales do not occur in June). The period of $\sim$60-h corresponds to the synoptic time scale in which atmospheric high and low pressure systems interchange. The 4-day time scale identified by Fourier analysis replicates this result.

The greatest instability of frequencies of the amplitude spectrum is characteristic of spring and 8–16-h cycles are pronounced. WT analysis revealed that for the entire period of the experiment the most significant aspect is the diurnal variation of concentration. However, as the cold season approaches, the amplitudes of 1-day oscillations decrease significantly and become less pronounced (Figure 6, upper). Thus, there is a certain relation between PNC and the intensity of solar radiation. The results of WT analysis of the peak values are comparable to those reported for the coast

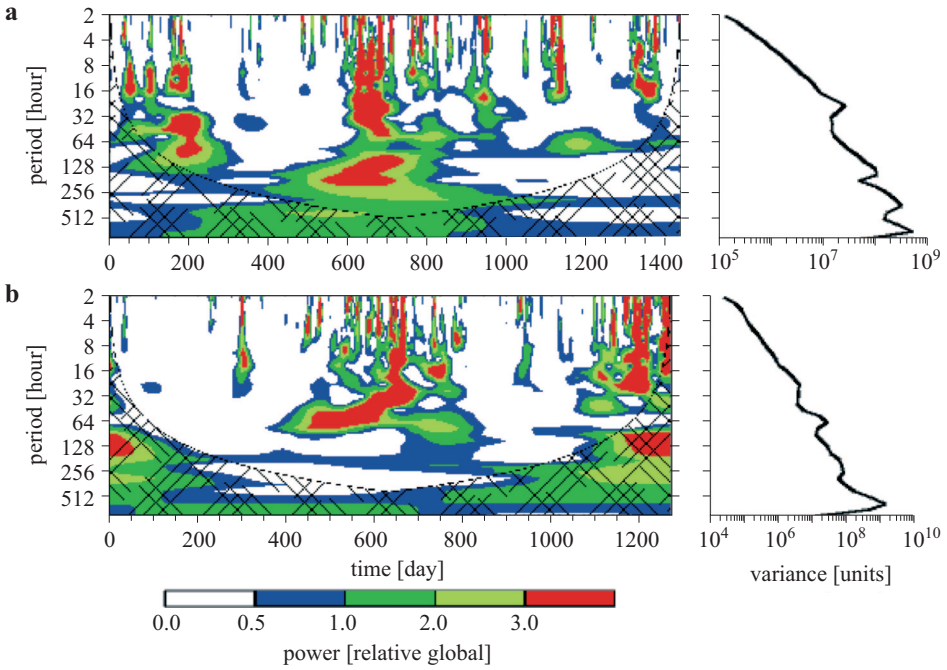

Figure 6. The wavelet power spectrum (using the Morlet wavelet) of aerosol particle number concentration (left) and global wavelet power spectrum (right): November–December (upper); April–May 2009 (bottom). The cross-hatched region is the cone of influence, where zero padding has reduced the variance in values of the first principal component

of Lake Baikal (Kaplinsky & Khutorova 2010), where periodicities of 4-, 6-, 12-, 14–16- and 22–24-h were detected. Mesoscale fluctuations can be caused by atmospheric dynamics associated with convection, relief, the daily variability of humidity and wind speed/direction and other meteorological parameters. The results were difficult to interpret owing to a variety of processes affecting the PNC. The presence of more oscillations during spring may indicate the existence of an effective synoptic mechanism influencing PNC dynamics. Analysis of the phase of the two-year period showed that the phase of the interval signal was not preserved. More attention was drawn to the existence and study of the period associated with new particle formation (3.3).

3.3.4. Pollutant concentration correlations

In order to investigate the characteristics and processes affecting PNC, together with meteorological parameters, trace gases were investigated at the Preila background marine site. Spearman correlation coefficients

Table 2. Spearman correlation coefficients between pollutant concentrations and meteorological parameters

	PNC	SO_2S	NO_2-N	NH_4+NH_3-N	NO_3+HNO_3-N	NO_3-N	NH_4-N	SO_4-S	Cl^-	Na^+	T	RH	UVR	Solar radiation
PNC	1	0.507^{**}	0.495^{**}	0.473^{**}	-0.565^{**}	-0.352^{**}	-0.093^{*}	-0.434^{**}	-0.443^{**}	-0.285^{**}	0.227^{**}	0.469^{**}	0.598^{**}	0.724^{**}
n		613	614	611	594	571	592	594	593	594	607	610	571	610
SO_2-S		1	0.353^{**}	0.321^{**}	-0.252^{**}	-0.307^{**}	-0.300^{**}	-0.386^{**}	-0.426^{**}	-0.211^{**}	-0.116^{**}	0.107^{**}	0.316^{**}	0.324^{**}
n			627	624	607	584	605	607	606	607	620	623	584	622
NO_2-N			1	0.659^{**}	-0.308^{**}	-0.082^{*}	-0.242^{**}	-0.375^{**}	-0.360^{**}	-0.374^{**}	-0.012	0.168^{**}	0.442^{**}	0.447^{**}
n				625	608	585	606	608	607	608	621	624	585	623
NH_4+NH_3-N				1	-0.246^{**}	-0.094^{*}	-0.008	-0.438^{**}	-0.388^{**}	-0.318^{**}	-0.035	0.170^{**}	0.303^{**}	0.414^{**}
n					606	583	604	606	605	606	619	622	582	620
NO_3+HNO_3-N					1	0.481^{**}	0.344^{**}	0.521^{**}	0.411^{**}	0.377^{**}	-0.312^{**}	-0.459^{**}	-0.530^{**}	-0.557^{**}
n						580	604	606	604	605	604	606	566	603
NO_3-N						1	0.427^{**}	0.329^{**}	0.329^{**}	0.148^{**}	-0.317^{**}	-0.378^{**}	-0.407^{**}	-0.413^{**}
n							579	581	579	580	583	584	545	582
NH_4-N							1	0.490^{**}	0.396^{**}	0.360^{**}	-0.135^{**}	-0.175^{**}	-0.261^{**}	-0.191^{**}
n								606	604	605	604	606	566	603
SO_4-S								1	0.688^{**}	0.541^{**}	-0.065	-0.265^{**}	-0.445^{**}	-0.458^{**}
n									606	607	606	608	569	605
Cl^-									1	0.619^{**}	0.014	-0.182^{**}	-0.372^{**}	-0.418^{**}
n										606	605	607	567	604
Na^+										1	0.047	-0.158^{**}	-0.335^{**}	-0.348^{**}
n											607	609	569	605
T											1	0.481^{**}	0.531^{**}	0.443^{**}
n												622	583	618
RH												1	0.650^{**}	0.589^{**}
n													585	621
UVR													1	0.757^{**}
n														582
Solar radiation														1

n – number of measurements; * – correlation significant at the 0.05 level; ** – correlation significant at the 0.01 level.

between PNC, meteorological parameters and trace gases are presented in Table 2. No strong correlation is found between NH_4-N and T. Nevertheless, there are statistically significant but weak correlations between PNC and nitrogen oxides, RH and UVR.

The Spearman correlation coefficients between Cl^- and $SO_4 - S$ were moderately good (0.68). Because $SO_4 - S$ is emitted from ships, a moderate correlation was expected with these pollutants, whereas there was a poor correlation between Na^+ and Cl^- as these ions originated from the sea. Similarly weak correlations were reported by Bukowiecki et al. (2002) between CO and ultrafine particle number concentrations.

4. Summary and conclusions

Two-year measurements of aerosol particle number concentrations were carried out in the south-eastern Baltic Sea region (Preila, Lithuania) during 2008–2009. The monthly mean variation of PNC showed high mean concentrations during the summer and early spring and low concentrations during winter. The long-range or regional transport of smoke emitted by wildfires had a strong impact on total aerosol number concentrations in Lithuania in the early spring. The lowest monthly PNCs were recorded during November 2008 (1500 ± 900 cm^{-3}) and the highest ones during June 2008 (4500 ± 900 cm^{-3}).

Variability in observed aerosol characteristics was found to coincide with changes in air mass source region, as indicated by back trajectories. The PSCF results for the marine environment showed that the Preila site is on an air parcel route in which PNCs are carried out over the Baltic Sea (17.9%) and southern Europe (39.3%). Principal Component Analysis confirmed that variations in the PNC diurnal patterns were due mainly to road traffic and combustion, as indicated by the high correlation between the concentrations of nitrogen oxides and the number concentrations of particles. Neglecting noise in the analysis, this correlation explains 46% of the total variance of the data. PCA clearly showed that PNC also depended strongly on UVR. In contrast to PC1, PC2 showed high loadings of Na^+, Cl^-, precipitation (2008) and wind speed (2009). This suggests that this component represents a general degree of marine influence.

The results of Fourier and wavelet transform analysis indicated that the most important variations in the data series were represented by periods of 4, 6–7, 11, 16 to 23 days, which could be attributable to synoptic scale fluctuations. For the entire period of the experiment the most significant aspect is the diurnal variation of particle number concentration. However, as the cold season approaches, the amplitudes of 1- and 2-day oscillations decrease significantly and become less pronounced.

Acknowledgements

We thank Mr Peter Senn for English editorial revision and valuable suggestions on how to improve this manuscript and the anonymous reviewers for their helpful comments.

References

Andriejauskienė J., Ulevicius V., Bizjak M., Špirkauskaitė N., Byčenkienė S., 2008, *Black carbon aerosol at the background site in the coastal zone of the Baltic Sea*, Lith. J. Phys., 48(2), 183–194, http://dx.doi.org/10.3952/lithjphys.48210.

Asmi A., Wiedensohler A., Laj P., Fjaeraa A.-M., Sellegri K., Birmili W., Weingartner E., Baltensperger U., Zdimal V., Zikova N., Putaud J.-P., Marinoni A., Tunved P., Hansson H.-C., Fiebig M., Kivekas N., Lihavainen H., Asmi E., Ulevicius V., Aalto P. P., Swietlicki E., Kristensson A., Mihalopoulos N., Kalivitis N., Kalapov I., Kiss G., de Leeuw G., Henzing B., Harrison R. M., Beddows D., O'Dowd C., Jennings S. G., Flentje H., Weinhold K., Meinhardt F., Ries L., Kulmala M., 2011, *Number size distributions and seasonality of submicron particles in Europe 2008–2009*, Atmos. Chem. Phys., 11 (11), 5505–5538, http://dx.doi.org/10.5194/acp-11-5505-2011.

Beddows D. C. S., Dall'Osto M., Harrison R. M., 2009, *Cluster analysis of rural, urban and curbside atmospheric particle size data*, Environ. Sci. Technol., 43 (13), 4694–4700, http://dx.doi.org/10.1021/es803121t.

Birmili W., Wiedensohler A., Plass-Dulmer C., Berresheim H., 2000, *Evolution of newly formed aerosol particles in the continental boundary layer: a case study including OH and H_2SO_4 measurements*, Geophys. Res. Lett., 27, 2205–2208, http://dx.doi.org/10.1029/1999GL011334.

Boy M., Kulmala M., 2002, *Nucleation events on the continental boundary layer: influence of physical and meteorological parameters*, Atmos. Chem. Phys., 2, 1–16, http://dx.doi.org/10.5194/acp-2-1-2002.

Bukowiecki N., Dommen J., Prevot A. S. H., Richter R., Weingartner E., Baltensperger U., 2002, *A mobile pollutant measurement laboratory-measuring gas phase and aerosol ambient concentrations with high spatial and temporal resolution*, Atmos. Environ., 36, 5569–5579, http://dx.doi.org/10.1016/S1352-2310(02)00694-5.

Byčenkienė S., Ulevicius V., Kecorius S., 2011, *Characteristics of black carbon aerosol mass concentration over the East Baltic region from two-year measurements*, J. Environ. Monitor., 13, 1027–1038, http://dx.doi.org/10.1039/c0em00480d.

Clarke A. D., Owens S. R., Zhou J. C., 2006, *An ultrafine sea-salt flux from breaking waves: Implications for cloud condensation nuclei in the remote marine atmosphere*, J. Geophys. Res., 111, D06202, http://dx.doi.org/10.1029/2005JD006565.

Dall'Osto M., Monahan C., Greaney R., Beddows D. C. S., Harrison R. M., Ceburnis D., O'Dowd C. D., 2011, *A statistical analysis of North East Atlantic*

(submicron) aerosol size distributions, Atmos. Chem. Phys., 11 (24), 12567–12578, http://dx.doi.org/10.5194/acp-11-12567-2011.

Delfino R. J., Staimer N., Tjoa T., Gillen D. L., Polidori A., Arhami M., Kleinman M. T., Vaziri N. D., Longhurst J., Sioutas C., 2009, *Air pollution exposures and circulating biomarkers of effect in a susceptible population: clues to potential causal component mixtures and mechanisms*, Environ. Health Persp., 117 (8), 1232–1238, http://dx.doi.org/10.1289/journla.ehp.0800194.

Dongarrá G., Manno E., Varrica D., Lombardo M., Vultaggio M., 2010, *Study on ambient concentrations of PM10, PM10–2.5, PM2.5 and gaseous pollutants. Trace elements and chemical speciation of atmospheric particulates*, Atmos. Environ., 44 (39), 5244–5257, http://dx.doi.org/10.1016/j.atmosenv.2010.08.041.

Einax J. W., Zwanziger H. W., Geiss S., 1997, *Chemometrics in environmental analysis*, VCH Verlagsgesellschaft mbH, Weinheim, 384 pp.

Englert N., 2004, *Fine particles and human health a review of epidemiological studies*, Toxicol. Lett., 149 (1–3), 235–242, http://dx.doi.org/10.1016/j.toxlet.2003.12.035.

Eskridge R., Ku J. Y., Rao S. T., Porter P. S., Zurbenko I. G., 1997, *Separating different time scales of motion in time series of meteorological variables*, B. Am. Meteorol. Soc., 78 (7), 1473–1483, http://dx.doi.org/10.1175/1520-0477(1997)078<1473:SDSOMI>2.0.CO;2.

Eskridge R., Ku J. Y., Rao S. T., Porter P. S., Zurbenko I. G., 1997, *Separating different time scales of motion in time series of meteorological variables*, B. Am. Meteorol. Soc., 78 (7), 1473–1483, http://dx.doi.org/10.1175/1520-0477(1997)078< 1473:SDSOMI>2.0.CO;2.

Fahrmeir L., Hamerle A., Tutz G., 1996, *Multivariate statistische Verfahren*, 2nd edn., de Gruyter, Berlin, 902 pp., (in Berlin).

Farge M., 2000, *Wavelet transform and their application to turbulence*, Ann. Rev. Fluid. Mech., 24, 395–457, http://dx.doi.org/10.1146/annurev.fl.24.010192.002143.

Foufoula-Georgiou E., Kumar P., 1995, *Wavelets in geophysics*, Elsevier, New York, 373 pp.

Gong K. W., Zhao W., Li N., Barajas B., Kleinman M. T., Sioutas C., Horvath S., Lusis A. J., Nel A. E., Araujo J. A., 2007, *Air-pollutant chemicals and oxidized lipids exhibit genome-wide synergistic effects on endothelial cells*, Genome Biol., 8 (7), R149, http://dx.doi.org/10.1186/gb-2007-8-7-r149.

Hies T., Treffeisen R., Sebald L., Reimer E., 2000, *Spectral analysis of air pollutants. Part 1: elemental carbon time series*, Atmos. Environ., 34 (21), 3495–3502, http://dx.doi.org/10.1016/S1352-2310(00)00146-1.

Hinds W. C., 1999, *Aerosol technology: properties, behavior and measurements of airborne particles*, 2nd edn., New York, Wiley Interscience, 509 pp.

Ho K. F., Lee S. C., Cao J. J., Li Y. S., Chow J. C., Watson J. G., Fung K., 2006, *Variability of organic and elemental carbon, water soluble organic*

carbon, and isotopes in Hong Kong, Atmos. Chem. Phys., 6, 4569–4576, http://dx.doi.org/10.5194/acp-6-4569-2006.

Jaenicke R., 1993, *Tropospheric aerosols*, [in:] *Aerosol-clouds-climate interaction*, P.V. Hobbs (ed.), Academic Press, San Diego, 1–31.

Jayaratne E. R., Verna T. S., 2001, *The impact of biomass burning on the environmental aerosol concentration in Gaborone, Botswana*, Atmos. Environ., 35 (10), 1821–1828, http://dx.doi.org/10.1016/S1352-2310(00)00561-6.

Juozaitis A., Trakumas S., Girgždienė R., Girgždys A., Šopauskienė D., Ulevicius V., 1996, *Investigations of gas-to-particle conversion in the atmosphere*, Atmos. Res., 41, 183–201, http://dx.doi.org/10.1016/0169-8095(96)00008-7.

Kaplinsky A. E., Khutorova O. G., 2010, *The wavelet analysis of aerosol characteristics at the Lake Baikal coast*, Polzunovskij vestnik, 1, 160–164, (in Russian).

Karaca F., Alagha O., Erturk F., 2005, *Statistical characterization of atmospheric PM10 and PM2.5 concentrations at a nonimpacted suburban site of Istanbul, Turkey*, Chemosphere, 59, 1183–1190, http://dx.doi.org/10.1016/j.chemosphere.2004.11.062.

Knutson T. R., Weickman K. M., 1987, *30–60 day atmospheric oscillations: composites of Convection and circulation anomalies*, Mon. Weather Rev., 115, 1407–1436, http://dx.doi.org/10.1175/1520-0493(1987)115<1407:DAOCLC>2.0.CO;2.

Kulmala M., Rannik U., Pirjola L., Dal Maso M., Karimaki J., Asmi A., Jappinen A., Karhu V., Korhonen H., Malvikko S. P., Puustinen A., Raittila J., Romakkaniemi S., Suni T., Yli-Koivisto S., 2000, *Characterization of atmospheric trace gas and aerosol concentrations at forest sites in southern and northern Finland using back trajectories*, Boreal Environ. Res., 5 (4), 315–336.

Kulmala M., Vehkamaki H., Petaja T., Dal Maso M., Lauri A., Kerminen V. M., Birmili W., McMurry P. H., 2004, *Formation and growth rates of ultrafine atmospheric particles: a review of observations*, J. Air Waste Manage., 35 (2), 143–176.

Laakso L., Hussein T., Aarnio P., Komppula M., Hiltunen V., Viisanen Y., Kulmala M., 2003, *Diurnal and annual characteristics of particle mass and number concentrations in urban, rural and Arctic environments in Finland*, Atmos. Environ., 37 (19), 2629–2641, http://dx.doi.org/10.1016/S1352-2310(03)00206-1.

Lohmann U., Feichter J., 2005, *Global indirect aerosol affects. A review*, Atmos. Chem. Phys., 5 (3), 715–737, http://dx.doi.org/10.5194/acp-5-715-2005.

Marr L. C., Harley R. A., 2002, *Spectral analysis of weekday-weekend differences in ambient ozone, nitrogen oxide, and non-methane hydrocarbon time series in California*, Atmos. Environ., 36 (14), 2327–2335, http://dx.doi.org/10.1016/S1352-2310(02)00188-7.

Moloi K., Chimidza S., Selin Lindgren E., Viksna A., Standzenieks P., 2002, *Black carbon mass and elemental measurements of airborne particles in the*

village of Serowe, Botswana, Atmos. Environ., 36 (14), 2447–2457, http://dx.doi.org/10.1016/S1352-2310(02)00085-7.

Mordas G., Kulmala M., Petäjä T., Aalto P. P., Matulevicius V., Grigoraitis V., Ulevicius V., Grauslys V., Ukkonen A., Hämeri K., 2005, *Design and performance characteristics of a condensation particle counter UF-02proto*, Boreal Environ. Res., 10 (6), 543–552.

Percival D. P., Walden A. T., 1998, *Spectral analysis for physical applications*, Cambridge Univ. Press, Cambridge, 612 pp.

Plauškaitė K., Ulevicius V., Špirkauskaitė N., Byčenkienė S., Zieliński T., Petelski T., Ponczkowska A., 2010, *Observations of new particle formation events in the south-eastern Baltic Sea*, Oceanologia, 52 (1), 53–75, http://dx.doi.org/10.5697/oc.52-1.053.

Putaud J.-P., Raes F., Van Dingenen R., Baltensperger J. P. U., Brüggemann E., Facchini M. C., Decesari S., Fuzzi S., Gehrig R., Hansson H. C., Hüglin C., Laj P., Lorbeer G., Maenhaut W., Mihalopoulos N., Müller K., Querol X., Rodriguez S., Schneider J., Spindler G., ten Brink H., Torseth K., Wehner B., Wiedensohler A., 2004, *European aerosol phenomenology – 2: chemical characteristics of particulate matter at kerbside, urban, rural and background sites in Europe*, Atmos. Environ., 38 (16), 2579–2595, http://dx.doi.org/10.1016/j.atmosenv.2004.01.041.

Rodriguez S., Van Dingenen R., Putaud J. P., Martins-Dos Santos S., Roselli D., 2005, *Nucleation and growth of new particles in the rural atmosphere of Northern Italy – relationship to air quality monitoring*, Atmos. Environ., 39 (36), 6734–6746, http://dx.doi.org/10.1016/j.atmosenv.2005.07.036.

Saliba N. A., El Jam F., El Tayar G., Obeid W., Roumie M., 2010, *Origin and variability of particulate matter (PM10 and PM2.5) mass concentrations over an Eastern Mediterranean city*, Atmos. Res., 97 (1–2), 106–114, http://dx.doi.org/10.1016/j.atmosres.2010.03.011.

Sardar S. B., Fine P. M., Yoon H., Sioutas C., 2004, *Associations between particle number and gaseous co-pollutant concentrations in the Los Angeles basin*, J. Air Waste Manage., 54 (8), 992–1005, http://dx.doi.org/10.1080/10473289.2004.10470970.

Torrence C., Compo G. P., 1998, *A practical guide to wavelet analysis*, B. Am. Meteorol. Soc., 79 (1), 61–78, http://dx.doi.org/10.1175/1520-0477(1998)079<0061:APGTWA>2.0.CO;2.

Ulevicius V., Byčenkienė S., Remeikis V., Garbaras A., Kecorius S., Andriejauskiene J., Jasinevičienė D., Mocnik G., 2010, *Characterization of pollution events in the East Baltic region affected by regional biomass fire emissions*, Atmos. Res., 98(2–4), 190–200, http://dx.doi.org/10.1016/j.atmosres.2010.03.021.

Ulevicius V., Byčenkienė S., Špirkauskaitė N., Kecorius S., 2010, *Biomass burning impact on black carbon aerosol mass concentration at a coastal site: case studies*, Lith. J. Phys., 50 (3), 335–344, http://dx.doi.org/10.3952/lithjphys.50304.

Ulevicius V., Zeromskiene K., Mordas G., 2001, *On the production of new particles in the Lithuanian coastal boundary layer*, J. Aerosol Sci., 32 (1), 605–606.

Verma V., Ning Z., Cho A. K., Schauer J. J., Shafer M. M., Sioutas C., 2009, *Redox activity of urban quasi-ultrafine particles from primary and secondary sources*, Atmos. Environ., 43, 6360–6368, http://dx.doi.org/10.1016/j.atmosenv.2009.09.019.

Vukovich F. M., 1997, *Time scales of surface ozone variations in the regional, non-urban environment*, Atmos. Environ., 31 (10), 1513–1530, http://dx.doi.org/10.1016/S1352-2310(96)00279-8.

Wilson J. G., Zawar-Reza P., 2006, *Intraurban-scale dispersion modeling of particulate matter concentrations: applications for exposure estimates in cohort studies*, Atmos. Environ., 40 (6), 1053–1063, http://dx.doi.org/10.1016/j.atmosenv.2005.11.026.

Xia T., Kovochich M. J., Brant J., Hotze M., Sempf J., Oberley T., Yeh J., Sioutas C., Wiesner M. R., Nel A. E., 2006, *Comparisons of the abilities of ambient and commercial nanoparticles to induce cellular toxicity according to an oxidative stress paradigm*, Nano Lett., 6 (8), 1794–1807, http://dx.doi.org/10.1021/nl061025k.